Electronic Surface Properties Hot Paper

International Edition: DOI: 10.1002/anie.201601824
German Edition: DOI: 10.1002/ange.201601824

Spatially Resolved Quantification of the Surface Reactivity of Solid Catalysts

*Bing Huang, Li Xiao, Juntao Lu, and Lin Zhuang**

Abstract: *A new property is reported that accurately quantifies and spatially describes the chemical reactivity of solid surfaces. The core idea is to create a reactivity weight function peaking at the Fermi level, thereby determining a weighted summation of the density of states of a solid surface. When such a weight function is defined as the derivative of the Fermi–Dirac distribution function at a certain non-zero temperature, the resulting property is the finite-temperature chemical softness, termed Fermi softness (S_F), which turns out to be an accurate descriptor of the surface reactivity. The spatial image of S_F maps the reactive domain of a heterogeneous surface and even portrays morphological details of the reactive sites. S_F analyses reveal that the reactive zones on a $Pt_3Y(111)$ surface are the platinum sites rather than the seemingly active yttrium sites, and the reactivity of the S-dimer edge of MoS_2 is spatially anisotropic. Our finding is of fundamental and technological significance to heterogeneous catalysis and industrial processes demanding rational design of solid catalysts.*

Structure-reactivity relationships are a core subject of all chemical research, and are of particular importance to heterogeneous catalysis,[1,2] a discipline that forms the foundation of many industrial processes, including those involving chemical production,[3,4] energy conversion,[5,6] and environmental remediation.[7,8] Given a molecular reactant or a solid catalyst, substance structure can be analyzed in atomistic detail with sophisticated physical methods, such as X-ray[9] spectroscopy, diffraction and imaging as well as electron-based techniques.[10] However, reactivity is a piece of chemical information that is not readily available for direct observation. To experimentally characterize the reactivity of a studied substance, external perturbations generally have to be induced. For instance, a test molecule may be used to probe how reactive the substance is. However, it would be much more convenient (and practically useful) if the reactivity of the studied substance could be directly and intrinsically described without involving these additional interactions. Efforts in this area of research have resulted in development of chemical reactivity theories,[11,12] such as the frontier molecular orbital (FMO) theory.[13]

Focusing on the highest occupied and lowest unoccupied molecular orbitals (HOMO and LUMO), FMO theory greatly simplifies the analysis of chemical reactivity and is able to provide a spatial description of the active site distribution on a molecule.[13,14] Besides, a number of electronic properties have been identified as the index, or descriptor, of chemical reactivity.[11] These include the electronegativity[15] and chemical hardness/softness,[16,17] well-known by chemists. These widely applied theories and concepts are designed for molecular systems but are not adequate for solid catalysts,[12,18] where a large number of frontier orbitals have to be dealt with.[19,20]

The chemical bonding on the surface of solids is much more complicated than that in discrete molecules. For a solid surface, not only the half-occupied Fermi level (E_F), but also the unoccupied states above E_F and the fully occupied states below E_F, interact with the HOMO and LUMO of the adsorbate[19] (Supporting Information, Figure S1). In other words, the whole frontier electronic band of the solid surface is reactive. Yet not every state in the band contributes equally to the surface bonding. Energy analyses reveal that the closer the state is to the E_F, the greater its contribution to bonding (Figure 1A; Supporting Information, Figure S1). Hence the reactivity of the solid surface should be determined by both the density of states ($g(E)$) and a weight function ($w(E)$)that quantifies the contribution of every state to the surface bonding. We hypothesized that the sum of all the weighted contributions ($\int g(E)w(E)dE$) would then act as a reactivity index of the solid surface (Figure 1B).

A crucial task is to find an appropriate form of the $w(E)$. Herein, we assign $w(E)$ to the derivative of the Fermi–Dirac distribution function[21] at a non-zero temperature, $-f'_T(E-E_F)$, which reaches a maximum at E_F and descends to zero as $|E-E_F|$ increases (Figure 1B; Supporting Information, Figure S2). The weighted sum of the reactivity contribution is then:

$$S_F = \int g(E)w(E)dE = -\int g(E)f'_T(E-E_F)dE \quad (1)$$

The resulting quantity (S_F) is termed the Fermi softness (that is, finite-temperature chemical softness), as it takes a form of the chemical softness (s) defined by density functional theory (DFT):[11]

$$s = \frac{\partial N}{\partial \mu} = \frac{\partial}{\partial E_F}\left[\int g(E)f_T(E-E_F)dE\right] \quad (2)$$

[*] B. Huang, L. Xiao, J. Lu, L. Zhuang
College of Chemistry and Molecular Sciences, Wuhan University
Wuhan 430072 (China)
E-mail: lzhuang@whu.edu.cn
L. Zhuang
Institute for Advanced Studies, Wuhan University
Wuhan 430072 (China)

Supporting information for this article, including Figure S1–S5 and Table S1 and S2, can be found under: http://dx.doi.org/10.1002/anie.201601824.

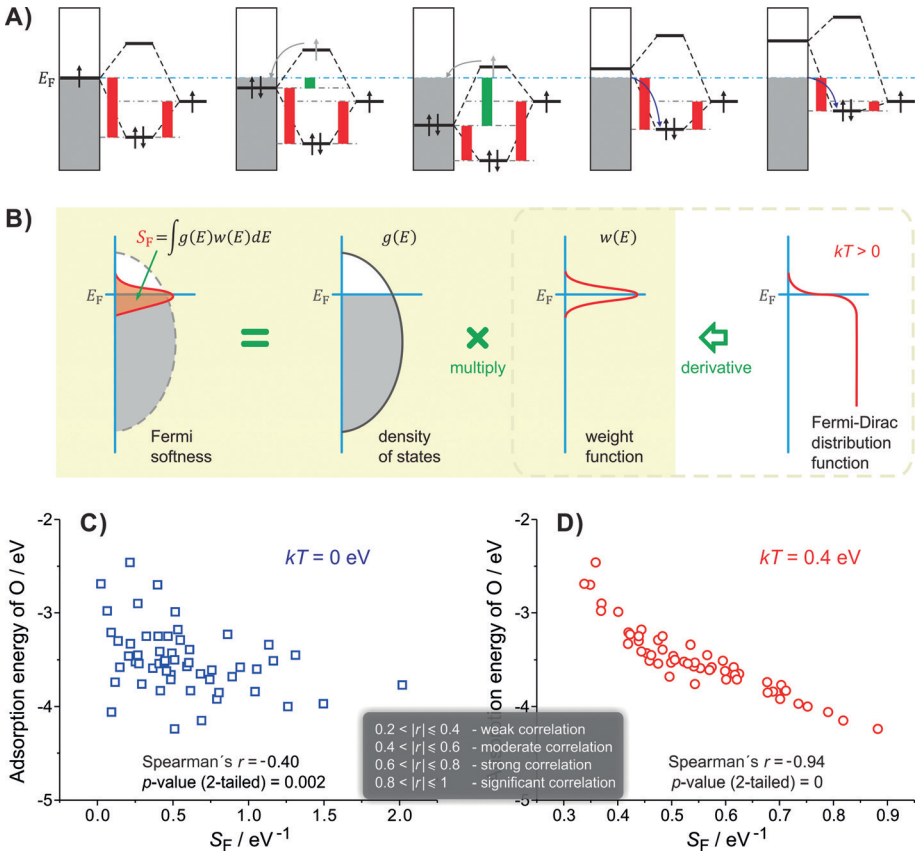

Figure 1. Definition of Fermi softness (S_F) and its correlation with surface reactivity. A) Energy analysis of surface bonding. Every state in the band, whether occupied or not, can contribute to the bonding; those closer to the Fermi level (E_F) are of more significance, as judged by the energy gain (red bar) and loss (green bar) on bonding (Supporting Information, Figure S1). B) S_F is defined as a weighted sum of the density of states $\int g(E)w(E)dE$, where the weight function $w(E)$ (peaking at the Fermi level) is taken in the present work to be the derivative of the Fermi–Dirac distribution function $-f'_T(E-E_F)$. C) Without spreading (that is, $kT=0$ eV), the S_F is the same as the density of states at Fermi level ($g(E_F)$), which does not correlate well with the surface reactivity (indicated here by the bonding with O_{ads}). D) By adjusting the nominal electronic temperature (for example, $kT=0.4$ eV), the S_F exhibits a significant correlation with the surface reactivity (Spearman's $r=-0.94$). Table S1 in the Supporting Information lists the adsorption energy data that were applied here.

where the chemical potential (μ) is replaced with E_F, the electron number N is calculated through an integral of the $g(E)$ with a Fermi–Dirac distribution at finite temperature,[12] and the derivative of $g(E)$ with respect to E_F is neglected.

The spreading of the $w(E)$ can be adjusted with the parametric temperature (T) or the nominal electron temperature (kT, where k is Boltzmann's constant; Supporting Information, Figure S2). To demonstrate the vital effect of $w(E)$ spreading, we use an adsorption energy dataset (Supporting Information, Table S1) to check the correlation between the resulting S_F and the surface reactivity. As displayed in Figure 1 C and D, the S_F at $kT=0$ eV, which is literally the density of states at Fermi level $g(E_F)$, shows a weak correlation with the surface bonding strength (Spearman's $r=-0.40$). In contrast, when kT is set to a non-zero value, 0.4 eV for example, the resulting S_F becomes significantly correlated with the surface reactivity (Spearman's $r=-0.94$). Systematic investigations show that significant correlation holds in a range of kT from 0.1 to 1 eV, and is optimal at 0.4 eV (for further examples of the correlation with surface reactivity see the Supporting Information, Figure S3).

The Fermi softness is an average property of the solid surface because the density of states ($g(E)$) is a global quantity averaged over the space. If the local density of states ($g(E,r)$) is used,[12] then the resulting Fermi softness,

$$S_F(r) = -\int g(E,r) f'_T(E-E_F)dE, \qquad (3)$$

becomes a local property of the solid surface, namely, a spatially resolved descriptor of the surface reactivity. Since $S_F(r)$ is a function of space, it can also be viewed as a chemical reactivity field over the solid surface.

The calculation of $S_F(r)$ is computationally low-cost. Given a solid surface with defined structure, the wave function of every energy eigenvalue ($\psi_E(r)$) can be obtained by a single-point DFT calculation. Using $g(E,r)=|\psi_E(r)|^2$, the $S_F(r)$ is then obtained by summing the weighted $g(E,r)$ values over an energy range $E_F \pm E_{cutoff}$ (see Experimental Section). Figure 2 displays calculated $S_F(r)$ maps for the closed packed surfaces of different transition metals, where the resulting $S_F(r)$ is projected onto an isosurface of charge density over the metal surface (the intensity of $S_F(r)$ is expressed chromatically). Note that the value of $S_F(r)$ (with the units keV^{-1} Å^{-3}) is absolute and comparable between different surfaces, although the scale of $S_F(r)$ in each image is specifically chosen for visual clarity.

Figure 2 clearly shows that the $S_F(r)$ of early transition metals is generally greater than that of late transition metals, and that the copper group is of the lowest reactivity, as expected. An important feature revealed by Figure 2 is that surface reactivity appears to be localized at the nucleus sites for late transition metals, while for early transition metals (in particular d^1–d^3) $S_F(r)$ tends to distribute in between the nuclei. These patterns are energetically reasonable because the early transition metal atoms tend to drive their scarce valence electrons into the bonding orbitals formed between atoms. Conversely, late transition metal atoms have excess valence electrons, which would fill in the non-bonding atomic orbitals (at E_F) localized at nuclei.

Such a spatially resolved quantification of surface reactivity is particularly valuable when the surface structure becomes heterogeneous. We demonstrate two examples in the

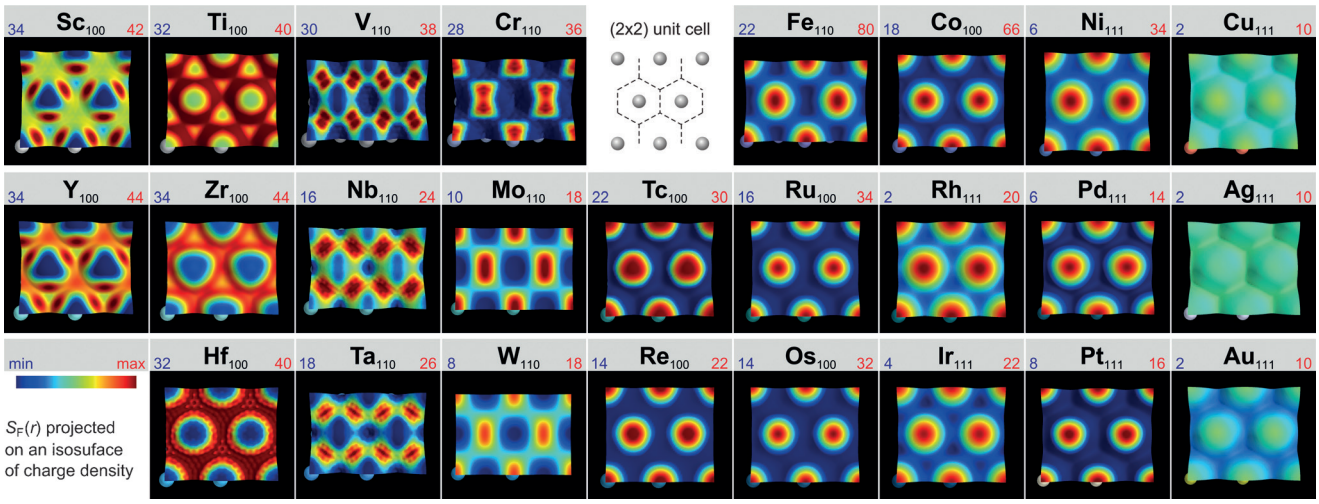

Figure 2. Local Fermi softness ($S_F(r)$) of the closed packed surfaces of transition metals. The $S_F(r)$ is projected onto an isosurface of charge density (under which 95% of the electronic charge resides). The quantity of $S_F(r)$ (with units, $keV^{-1}Å^{-3}$) is described by a color range (minimum and maximum are labeled at the left-top and the right-top of each image, respectively). The $S_F(r)$ for manganese is not presented because of the lack of closed packed surface.

following discussion. The first one is a Pt_3Y intermetallic surface.[22] As depicted by the insets of Figure 3A, the Y(001) and Pt(111) surfaces show an $S_F(r)$ pattern typical of early and late transition metals, respectively. Even the weakest domain of $S_F(r)$ on yttrium is much greater in magnitude than the strongest part of $S_F(r)$ on platinum, meaning that the pure yttrium surface is far more active than the pure platinum surface. When mixing these two elements, the $Pt_3Y(111)$ surface displays an entirely different $S_F(r)$ picture. As shown in Figure 3A, the high S_F value spot appears at the platinum site, while the yttrium site is of significantly lower activity.

The $S_F(r)$ analysis of $Pt_3Y(111)$ indicates that the platinum site is more reactive than the yttrium site, despite the equal charge density in space. This observation is contrary to our chemical intuition, but is not difficult to verify. Herein, we test the binding strength of seven typical adsorbates at platinum and yttrium sites. As illustrated in Figure 3B, the adsorption energies are all greater in magnitude on platinum, despite the chemical differences between these probe species. The fact that the reactivity difference between sites varies with specific adsorbates is understandable, as the electronic character of the surface would be perturbed to different degrees upon adsorption. Nonetheless, the $S_F(r)$ results correctly portray the peculiar reactivity of the $Pt_3Y(111)$ surface, which cannot be achieved with other properties, such as the well-known *d*-band center.[23] Specifically, based on the projected density of states (PDOS; Figure 3C), the *d*-band center of the surface yttrium atom is higher than that of the platinum atom, indicating that the yttrium sites should be more reactive. However, this is not the case.

The second example used to demonstrate the power of $S_F(r)$ employs a more complicated structure; a one-dimensional MoS_2 edge, which has been identified as the local structure responsible for the high catalytic activity of the material in the hydrogen evolution reaction (HER).[24] In this structure (Figure 4A), the chemical environment comprises three types of sulfur atoms (S#1, S#2, and S#3) and two types of molybdenum atoms (Mo#1 and Mo#2). The periodic S#1 dimer is the reactive edge of interest,[25] displaying a sharp $g(E)$ peak at E_F (Figure 4B), resulting in an S_F significantly greater than that of the other sulfur species The three-dimensional view of the $S_F(r)$ (Figure 4C; Supporting Information, Figure S4) provides a spatially precise depiction of the chemical reactivity of the whole MoS_2 edge. Although both Mo#1 and Mo#2 exhibit a d_{z^2} orbital-like $S_F(r)$

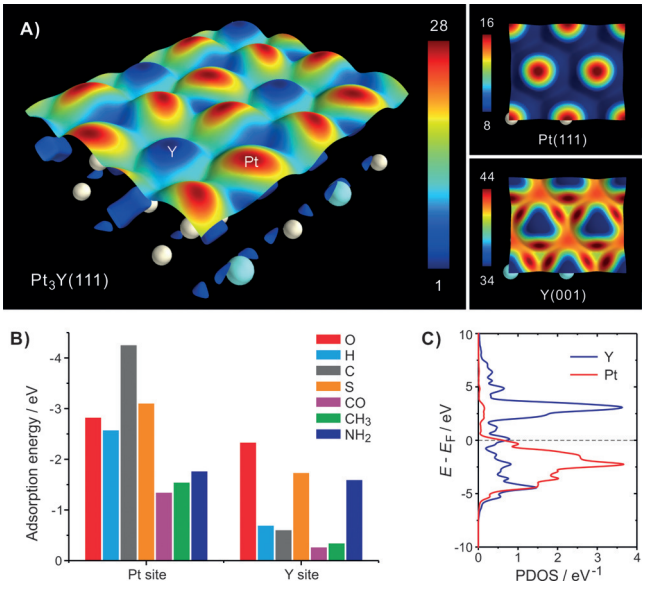

Figure 3. Spatially resolved quantification of the chemical reactivity of a Pt_3Y alloy surface. A) The local Fermi softness ($S_F(r)$) of the $Pt_3Y(111)$ surface is projected onto an isosurface of charge density (under which 95% of the electronic charge resides). The quantity of $S_F(r)$ (with units, $keV^{-1}Å^{-3}$) is described chromatically. $S_F(r)$ of Pt(111) and Y(001) are also presented for comparison. B) Examination of the reactivity of the platinum and yttrium site on $Pt_3Y(111)$ by comparison of their binding strengths with various adsorbates. C) The projected density of states (PDOS) of the platinum and yttrium atoms at the first layer of the $Pt_3Y(111)$ surface, showing that neither the vacancy number nor the *d* band center can serve as a reactivity index for this alloy system.

(with orientations orthogonal with respect to each other), the reactivity of the molybdenum species is concealed because it is surrounded by sulfur atoms. On the other hand, the $S_F(r)$ of S#1 is exposed and resembles a tilted p orbital, in comparison to the small-sized $S_F(r)$ of S#3 and the almost invisible $S_F(r)$ of S#2 (Figure 4C and D).

The tilted $S_F(r)$ of S#1 reveals previously unknown, subtle information: the reactivity of the S#1 dimer edge is spatially anisotropic. Specifically, although all S#1 atoms are in the same chemical environment, with the length of an S#1 dimer (3.06 Å) slightly shorter than the distance between two S#1 dimers (3.22 Å; see Figure 4D), the tilted $S_F(r)$ makes the reactivity field over an S#1 dimer stronger than that between two S#1 dimers. In particular, the distance between the crown of $S_F(r)$ of two S#1 sites is about 1–2 Å (inset of Figure 4D), a space configuration that is ideal for catalyzing a two-center reaction. To ascertain that such a fine structure of surface reactivity does affect the catalysis, we compared the reaction energy barrier of H–H bond formation ($2H_{ad} \rightarrow H_2$) over two different bridge sites on the S#1 dimer edge, namely the intra-dimer (br–y) and inter-dimer (br–x) sites (Figure 4E). The NEB (nudged elastic band) calculations clearly show that H–H bond formation catalyzed by a single S#1 dimer has a lower energy barrier (1.2 eV) than that for two S#1 dimers (1.9 eV). This observation is consistent with the anisotropic reactivity picture offered by the $S_F(r)$.

In conclusion, Fermi softness is proposed as a readily obtainable electronic property of the solid surface, which is quantitatively related to the surface reactivity and also allows reactivity imaging with atomistic resolution (for further examples see the Supporting Information, Figure S5, where the S_F of N-doped graphene indicates that the most activated sites are carbon atoms located next to the nitrogen dopant. This observation is consistent with recently reported[26] experimental observations). These advanced functionalities are of vital importance to the study of solid catalysts, but have not been fully implemented by previously reported methods (for example, the Fukui function cannot be directly applied to solids, whereas the *d*-band center method has no function in reactivity imaging). The findings presented in this paper will further the fundamental understanding of solid state chemistry and promote rational design of heterogeneous catalysts for industrial applications.

Experimental Section

Density functional theory (DFT) calculations were performed using the DACAPO code.[27] Ultrasoft pseudopotentials were used to describe the ionic cores and the plane wave cut-off energy was set to 408 eV (30 Ry). The effects of exchange and correlation interaction were described by the GGA-PW91 functional.

For the calculations of transition metal surfaces, a 2×2 surface unit cell was used to construct a four-layer metal slab that was then repeated in supercell geometry with successive slabs separated by a vacuum region equivalent to six metal layers. Adsorption was allowed on only one of the two exposed surfaces, and dipole correction was turned on to account for the resulting asymmetry effects. The adsorbate layer and the top two layers of the metal slab were allowed to relax until the forces acting on each non-constrained

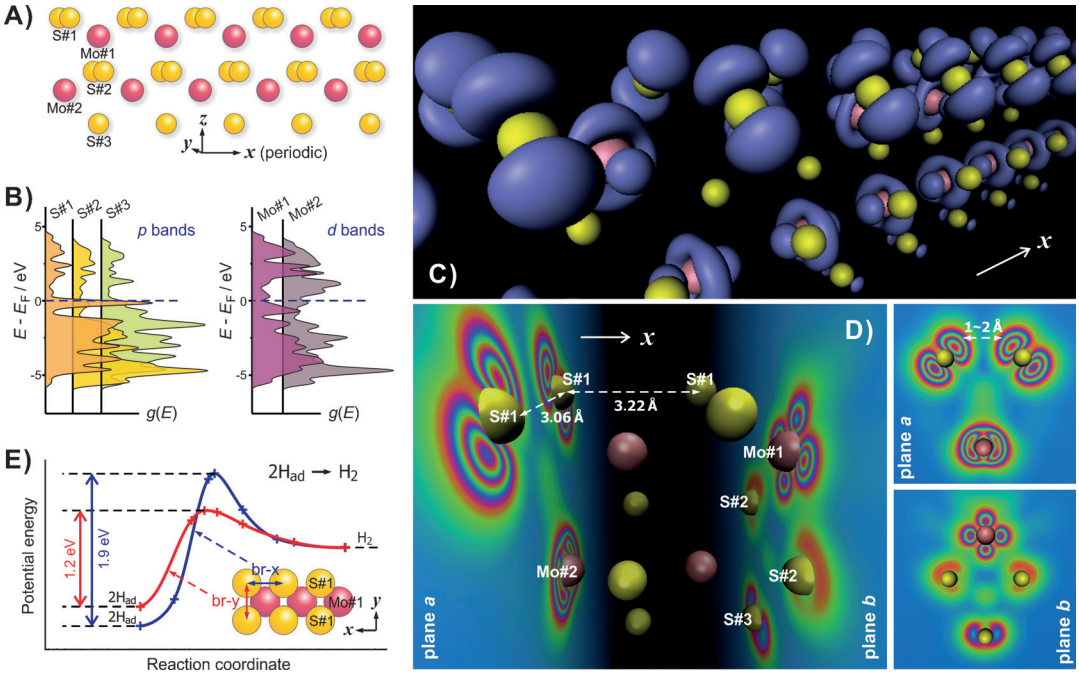

Figure 4. Spatially precise depiction of the chemical reactivity of a one-dimensional MoS_2 edge. A) The computational model, involving three types of sulfur atoms (S#1, S#2, and S#3) and two types of molybdenum atoms (Mo#1 and Mo#2). B) The density of states ($g(E)$) projected onto specific sulfur and molybdenum atoms. C) A three-dimensional view of the calculated $S_F(r)$ isosurface (blue, on which $S_F = 55$ keV^{-1} Å^{-3}); see Figure S4 in the Supporting Information for more views from alternative perspectives. D) The $S_F(r)$ is projected onto two planes normal to the x direction: plane *a* intersects two S#1 and one Mo#2 atoms, and plane *b* contains one Mo#1, two S#2, and one S#3 atoms. E) The difference in energy barrier for the $2H_{ad} \rightarrow H_2$ reaction at two kinds of bridge sites (br–x or br–y, as indicated by the inset) on the S#1 dimer edge, obtained from NEB (nudged elastic band) calculations.

atom were less than 0.05 eV Å^{-1}. Fermi–Dirac occupation statistics were employed to smear the electronic states around the Fermi level and the corresponding electronic temperature was set to 0.1 eV. The first Brillouin zone was sampled by a $6\times6\times1$ mesh using the Monkhorst-Pack scheme.[28]

The structure of MoS_2 adopted in the present work was similar to that in the literature[29] and mimics the STM-observed edge structure of MoS_2 on Au(111).[24] Parameters for geometry optimization were set the same as for metal surfaces, except that a *k*-point mesh of $12\times1\times1$ was used.

Fermi softness calculation: In this paper, global Fermi softness (S_F) was presented prior to the local Fermi softness ($S_F(r)$). In practice the calculation process was inversed: the $S_F(r)$ was first calculated using Eq. 3, and S_F then obtained by integrating the $S_F(r)$ over space. After DFT calculations were performed for a given structure, the local density of states ($g(E,r)$) was calculated by summing the absolute square of the wave functions under the same eigenenergy (E), $|\psi(E,r)|^2$. The resulting $g(E,r)$ was then multiplied with the weight function (that is, the derivative of the Fermi–Dirac function; $-f'_T(E-E_F)$), and then integrated over an energy range $E_F \pm E_{cutoff}$ to produce the $S_F(r)$. E_{cutoff} was determined by $-f'_T(E_{cutoff}-E_F) < 0.001$, that is, the weight of any reactive eigenstate should be greater than 0.1 %.

The $S_F(r)$ was stored in a cube-format file, and can be visualized using software such as Mayavi. To calculate the averaged S_F of a surface, the $S_F(r)$ was integrated over the space of the first atomic layer of the surface. In the present work, we applied Bader's scheme[30] to determine the volume of surface atoms and integrated the $S_F(r)$ within that volume to get S_F.

The S_F at zero electronic temperature, that is, the density of states at Fermi level ($g(E_F)$), was calculated for comparison. Sufficient accuracy was ensured by minimizing Fermi smearing in the DFT calculation (0.01 eV for example). The *k*-point sampling was raised to $12\times12\times1$ for a 2×2 unit cell of the metal surface, such that the obtained single-energy level was very close to the Fermi level with a discrepancy less than 0.01 eV.

Acknowledgements

We thank Prof. John Varcoe (University of Surrey, UK) for proofreading the English of this paper. This work was financially supported by the National Basic Research Program (2012CB932800, 2012CB215503), the National Natural Science Foundation (21125312, 91545205), and the 111 project (111-2-10).

Keywords: density functional calculations · heterogeneous catalysis · surface reactivity · density of states · Fermi softness

How to cite: *Angew. Chem. Int. Ed.* **2016**, *55*, 6239–6243
Angew. Chem. **2016**, *128*, 6347–6351

[1] For details about heterogeneous catalysis, see: R. Schlögl, *Angew. Chem. Int. Ed.* **2015**, *54*, 3465–3520; *Angew. Chem.* **2015**, *127*, 3531–3589.
[2] For further details about heterogeneous catalysis, see: N. Mizuno, M. Misono, *Chem. Rev.* **1998**, *98*, 199–217.
[3] C. W. Li, J. Ciston, M. W. Kanan, *Nature* **2014**, *508*, 504–507.
[4] X. Guo, et al., *Science* **2014**, *344*, 616–619.
[5] X. Huang, et al., *Science* **2015**, *348*, 1230–1234.
[6] S. Hu, et al., *Science* **2014**, *344*, 1005–1009.
[7] I. X. Green, W. Tang, M. Neurock, J. T. Yates, *Science* **2011**, *333*, 736–739.
[8] X. Xie, Y. Li, Z.-Q. Liu, M. Haruta, W. Shen, *Nature* **2009**, *458*, 746–749.
[9] J. Gustafson, et al., *Science* **2014**, *343*, 758–761.
[10] M. Azubel, et al., *Science* **2014**, *345*, 909–912.
[11] For details about conceptual Density Functional Theory, see: P. Geerlings, F. De Proft, W. Langenaeker, *Chem. Rev.* **2003**, *103*, 1793–1874.
[12] W. Yang, R. G. Parr, *Proc. Natl. Acad. Sci. U.S.A.* **1985**, *82*, 6723–6726.
[13] K. Fukui, *Science* **1982**, *218*, 747–754.
[14] P. W. Ayers, R. G. Parr, *J. Am. Chem. Soc.* **2000**, *122*, 2010–2018.
[15] R. S. Mulliken, *J. Chem. Phys.* **1934**, *2*, 782–793.
[16] R. G. Parr, R. G. Pearson, *J. Am. Chem. Soc.* **1983**, *105*, 7512–7516.
[17] L. T. Nguyen, F. De Proft, M. C. Amat, G. Van Lier, P. W. Fowler, P. Geerlings, *J. Phys. Chem. A* **2003**, *107*, 6837–6842.
[18] S. Wilke, M. H. Cohen, M. Scheffler, *Phys. Rev. Lett.* **1996**, *77*, 1560–1563.
[19] R. Hoffmann, *Rev. Mod. Phys.* **1988**, *60*, 601–628.
[20] N. Sablon, F. De Proft, P. Geerlings, *J. Chem. Theory Comput.* **2009**, *5*, 1245–1253.
[21] Fermi–Dirac distribution function is defined as: $f_T(E-E_F) = \{\exp[(E-E_F)/kT]+1\}^{-1}$.
[22] J. Greeley, et al., *Nat. Chem.* **2009**, *1*, 552–556.
[23] B. Hammer, J. K. Nørskov, *Nature* **1995**, *376*, 238–240.
[24] T. F. Jaramillo, et al., *Science* **2007**, *317*, 100–102.
[25] M. V. Bollinger, et al., *Phys. Rev. Lett.* **2001**, *87*, 196803.
[26] D. Guo, R. Shibuya, C. Akiba, S. Saji, T. Kondo, J. Nakamura, *Science* **2016**, *351*, 361–365.
[27] For details refer to: Dacapo,Dacapo, https://wiki.fysik.dtu.dk/dacapo.
[28] H. J. Monkhorst, J. D. Pack, *Phys. Rev. B* **1976**, *13*, 5188–5192.
[29] C. Tsai, F. Abild-Pedersen, J. K. Nørskov, *Nano Lett.* **2014**, *14*, 1381–1387.
[30] W. Tang, E. Sanville, G. Henkelman, *J. Phys. Condens. Matter* **2009**, *21*, 084204.

Received: February 22, 2016
Published online: April 13, 2016

